

Article

Open-Source Equipment Design for Cost-Effective Redox Flow Battery Research

Trinh V. Dung¹, Nguyen T. T. Huyen¹, Nguyen L. T. Huynh^{2,3}, Nguyen T. Binh¹, Nguyen T. Dat¹ ,
Nguyen T. T. Nga¹, Nguyen T. Lan¹, Hoang V. Tran¹ , Nguyen T. T. Mai¹ and Chinh D. Huynh^{1,*}

¹ School of Chemical Chemistry and Life Science, Hanoi University of Science and Technology, Hanoi 100000, Vietnam; genji0306@gmail.com (T.V.D.); huyen.nguyenthithu@hust.edu.vn (N.T.T.H.); nguyentaibinh0109@gmail.com (N.T.B.); datnt147@gmail.com (N.T.D.); nga.nguyenthithuy@hust.edu.vn (N.T.T.N.); lan.nguyenthi@hust.edu.vn (N.T.L.); hoang.tranvinh@hust.edu.vn (H.V.T.); mai.nguyenthituyet@hust.edu.vn (N.T.T.M.)

² Faculty of Chemistry, University of Science, 227 Nguyen Van Cu Street, Ho Chi Minh City 700000, Vietnam; hltnguyen@hcmus.edu.vn

³ Viet Nam National University Ho Chi Minh City, Thu Duc City, Ho Chi Minh City 700000, Vietnam

* Correspondence: chinh.huynhdang@hust.edu.vn

Abstract: Redox flow batteries (RFBs), with distinct characteristics that are suited for grid-scale applications, stand at the forefront of potential energy solutions. However, progress in RFB technology is often impeded by their prohibitive cost and the limited availability of essential research and development test cells. Addressing this bottleneck, we present herein an open-source device tailored for RFB laboratory research. Our proposed device significantly lowers the financial barriers to research and enhances the accessibility of vital equipment for RFB studies. Employing innovative fabrication methods such as laser cutting, 3D printing, and CNC machining, a versatile and efficient flow cell has been designed and fabricated. Furthermore, our open laboratory research equipment comprises the Opensens potentiostat, charge/discharge testing devices, peristaltic pumps, and inexpensive rotating electrodes. Every individual element contributes significantly to the establishment of an all-encompassing experimental configuration that is both economical and efficient, thereby facilitating expedited progress in RFB research and development.

Keywords: open source; Opensens; redox flow battery (RFB); vanadium (V) oxide (V₂O₅); vanadium (IV/V) ions; cerium (III/IV) ions; electrolyte



Citation: Dung, T.V.; Huyen, N.T.T.; Huynh, N.L.T.; Binh, N.T.; Dat, N.T.; Nga, N.T.T.; Lan, N.T.; Tran, H.V.; Mai, N.T.T.; Huynh, C.D. Open-Source Equipment Design for Cost-Effective Redox Flow Battery Research.

ChemEngineering **2024**, *8*, 120.

<https://doi.org/10.3390/chemengineering8060120>

Academic Editor: Pengcheng Du

Received: 30 May 2024

Revised: 13 November 2024

Accepted: 19 November 2024

Published: 28 November 2024



Copyright: © 2024 by the authors. Licensee MDPI, Basel, Switzerland. This article is an open access article distributed under the terms and conditions of the Creative Commons Attribution (CC BY) license (<https://creativecommons.org/licenses/by/4.0/>).

1. Introduction

Integrating renewable energy sources into the grid is becoming more important due to the requirements of mitigating climate change and reducing dependence on finite fossil fuel reserves [1,2]. Renewable sources such as wind, solar, and hydroelectric power offer a sustainable and environmentally friendly means of electricity generation [3]. However, their intermittent and unpredictable nature poses a significant challenge to the stability and reliability of the electrical grid [4]. This intermittency results from fluctuations in weather conditions and diurnal patterns, making it imperative to have a reliable means of storing the excess energy generated during favorable conditions for later use when generation is low [5]. Large-scale energy storage systems have emerged as a pivotal solution to address this challenge by enabling the efficient capture and release of renewable energy, thereby ensuring grid stability and a consistent power supply [6].

Among the diverse technologies vying for the role of large-scale energy storage, redox flow batteries (RFBs) have garnered substantial research attention due to their unique attributes and promising prospects for grid-scale applications [7,8]. RFBs distinguish themselves by decoupling power and energy, a feature that grants them unparalleled flexibility in matching power output with energy capacity. This capability allows RFBs to

be tailored to suit diverse grid requirements, rendering them highly adaptable to varying grid demands [9]. Additionally, RFBs exhibit commendable longevity, outperforming certain conventional energy storage technologies in terms of operational lifespan [10–12]. Furthermore, the utilization of liquid electrolytes in RFBs enhances their chemical stability, thereby reducing degradation over time. These advantages collectively position redox flow batteries as a promising and robust technology for large-scale energy storage, offering a compelling solution to facilitate the seamless integration of renewable energy sources into the grid.

The challenges and limitations associated with current redox flow battery test cells are multifaceted, encompassing issues such as high cost, low reliability, and suboptimal performance [13]. Researchers have actively sought solutions to these challenges, primarily focusing on the development of novel electrolyte and membrane technologies [14]. Still, the test cells that are used to see how well these new ideas work often have big problems, like being very expensive and not being easy to change. These problems could make it hard to break into the field of flow battery research.

Usually, commercially available test cells with active areas of about 6 cm² cost around USD 1000 [15,16]. There are also sometimes problems with the seals on these cells. Additionally, the equipment needed for research into redox flow batteries is very expensive and includes circulating pumps with controllers and testing devices [17,18]. To address these cost and accessibility concerns, this study introduces an open-design approach for the fabrication of essential equipment for redox flow battery laboratory research, incorporating methods such as laser cutting, 3D printing [19], and CNC machining, thereby enhancing the accessibility and affordability of critical tools for advancing research in this field.

2. Materials and Methods

2.1. Flow Cell Fabrication

Many manufacturing and design procedures have been significantly transformed by rapid prototyping tools. While laser cutting is renowned for its speed and accuracy in producing intricate designs, its application is restricted to flat materials, and the process can be quite expensive. In contrast, CNC (computer numerical control) machining is precise and versatile, but its subtractive nature results in material waste and necessitates specialized operation. Lastly, 3D printing distinguishes itself by enabling the creation of complex geometries.

2.1.1. Membrane Preparation

The Nafion N212 membrane was customized to fit the specific dimensions of each cell design. To remove organic impurities, the membrane was subjected to a one-hour boiling process in a solution containing 5% hydrogen peroxide (H₂O₂) at 80 °C. Subsequently, the membrane was cleansed thoroughly with deionized water and submerged once more in 80 °C water for 1 h to guarantee the total elimination of residual H₂O₂. Finally, the membrane was treated with 1.0 M of sulfuric acid (H₂SO₄) solution at 80 °C.

2.1.2. Build Instruction

Components (required parts):

- 2 × Teflon end plates.
- 2 × Current collectors.
- 4 × Silicon plates.
- 2 × 45 × 45 mm Graphite sheets.
- 1 × Nafion membrane sheet.
- 2 × Vertical channels (mica plate).
- 2 × Horizontal channels (silicon).
- 2 × 25 × 25 mm pieces of graphite felt.
- 4 × M4 Stainless-steel 304 bolts.
- 4 × M4 Stainless-steel 304 hex nuts.

- 4 × M4 304 Silicon gaskets.

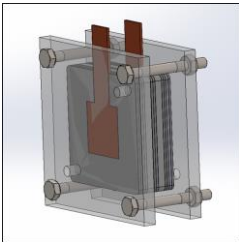
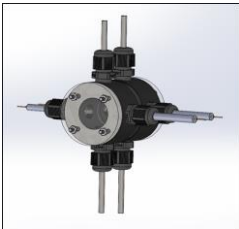
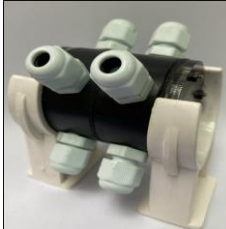
2.1.3. Assembly Steps

1. The following components should be assembled: 2 Teflon end plates, 2 current collectors, 4 silicon plates, 2 graphite sheets (45 × 45 mm), 1 Nafion membrane sheet, 2 vertical channels (mica plate), 2 horizontal channels (silicon), 2 pieces of graphite felt (25 × 25 mm), 4 M4 stainless steel 304 bolts, 4 M4 stainless steel 304 hex nuts, and 4 M4 304 silicon gaskets.
2. Attach the silicon gaskets and current collectors securely to the Teflon end plates.
3. On each current collector, layer the components as follows: first, a graphite sheet is positioned, followed by a horizontal channel, and then a vertical channel.
4. Insert a graphite felt piece into the middle of the vertical channel, ensuring that it fits snugly.
5. Carefully place the Nafion membrane on top of the assembled components, ensuring proper alignment.
6. Repeat the same assembly process for the remaining half-cell, following steps 2 through 5, but omit the Nafion membrane.
7. Securely tighten the screws to firmly hold the assembled components in place, creating two half-cells.
8. Attach the necessary tubing for the electrolyte inlet and outlet, ensuring proper connections for the flow of the electrolyte within the test cell.

2.1.4. Cell Design Variations

Various cell designs have been fabricated; the appropriate accessories for fabrication of the designed cells are listed in Table S1 of Supporting Information S1 (SI 1). The two cell designs that have been used for fabrication of the RFBs described in this work are shown in Table 1.

Table 1. Designed flow cells for laboratory use.

No.	Type	CAD Image	Digital Photos of Samples	Application	Link
2	Lab cell			True redox flow batteries (Fe-Cr, All-V, V-Ce, ...)	Lab 1b (https://github.com/huongnt212/OPENSENS-RFB-Research/blob/main/Flow%20cell%20design%20for%20Lab/Lab1b.STEP)
5	Flow cell			Flow cell for electrochemical purposes	Flow cell 1a (https://github.com/huongnt212/OPENSENS-RFB-Research/blob/main/Flow%20cell%20design%20for%20Lab/Flow_cell_1a.STEP)

This paper describes several unique designs that are adapted to different types of research in the field of battery technology and electrochemistry. This variability of research requirements requires the customization of the flow cell's design and geometry. Each of these designs represents a particular adaptation of the open-source flow cell concept, demonstrating the flexibility and adaptability of this approach for meeting diverse research needs:

- **Flow Cell for All Liquid Electrolyte Research:** This design is optimized for studies involving entirely liquid electrolytes. It is structured to facilitate the investigation of various liquid electrolyte chemistries and their interactions within the flow cell environment. This versatility makes it an ideal choice for a broad range of liquid electrolyte-based redox flow battery research.
- **Hybrid Flow Cell for Zn-Br Research:** Specifically designed for zinc-bromine battery systems, this hybrid flow cell accommodates the unique demands of Zn-Br research. The cell addresses the specific electrochemical and physical characteristics of zinc-bromine chemistries, making it a crucial tool for advancing research in this area.
- **H-Cell for Electrochemical Research:** The H-cell design is particularly useful for fundamental electrochemical studies. Its configuration allows for a clear separation of the anode and cathode chambers, providing a controlled environment for studying electrochemical reactions and processes in isolation.
- **Hybrid Air-Liquid Flow Cell:** This innovative design is tailored for research involving air-breathing electrodes or systems where gas-liquid interactions are crucial. It is particularly relevant for studying systems like metal-air batteries, where the interaction between the liquid electrolyte and the gaseous phase plays a critical role in the battery's operation and efficiency.

2.2. Chemicals and Reagents

Various chemicals and reagents were used, including vanadium pentoxide (V_2O_5 , 99.5 wt.%), Oxalic acid dihydrate ($C_2H_2O_4 \cdot 2H_2O$, 99.5 wt.%), sulfuric acid (H_2SO_4 , 98 wt.%), cerium (III) carbonate hydrate ($Ce_2(CO_3)_3 \cdot xH_2O$, wt. 99%), methanesulfonic acid (CH_4O_3S , wt. 99%) and L-Lysine ($HOOCC(CH_2)_4NH_2$, wt. 98.5%).

2.3. RFB Charge/Discharge Testing

Charge/discharge testing devices play a pivotal role in redox flow battery (RFB) research, primarily by enabling a deeper understanding of the working characteristics of these systems. These devices are essential for evaluating the operational efficiency, durability, and overall performance of RFBs under various conditions. By simulating real-world scenarios, they help researchers assess how RFBs respond to different charging and discharging cycles, which is crucial for optimizing their design and functionality. However, the development and availability of specific charge/discharge testing devices for RFB research are limited. This limitation stems from the unique challenges associated with the variability in potential and current seen during RFB cycling. RFBs often exhibit a wide range of operational voltages and currents, which can differ significantly from other battery types like NiMH or lithium-ion batteries. This variability poses a challenge in accurately measuring and analyzing the performance of RFBs using standard commercial testing devices, which are typically designed with the characteristics of more conventional battery technologies.

For single cells with a small working electrode area, a commercial charge/discharge testing device for lithium-ion batteries can be used for redox flow battery research, with careful setup and monitoring.

However, there is a drawback to using commercial testing devices for the testing of multiple-cell configurations or large-surface-area RFB cells, which result in high-voltage outputs or may require handling high currents. Commercial testing devices often fall short in accommodating these high voltage or current requirements, making it difficult to thoroughly evaluate the performance of such RFB systems. This gap in testing capability highlights the need for more specialized and adaptable charge/discharge testing devices that are tailored to the unique requirements of RFB research. Hence, the charge/discharge testing module that was designed and produced by the research team is a critical component in the evaluation of redox flow batteries and has been designed with two distinct boards: the power module board and the ESP32-IO connection board.

The power module board forms the core of this system, directly interfacing with the battery stack and a programmable power source (PPS). It is equipped to handle a

substantial range of electrical input and output and is capable of monitoring voltages from 0 to 10 volts and current up to ± 200 amperes. This wide range allows for comprehensive testing across various battery configurations and operating conditions, ensuring accurate and reliable data on battery performance during both charge and discharge cycles.

Complementing the power module, the ESP32-IO connection board has been designed with an array of input and output capabilities (Figure 1). It features 8 analog inputs and 12 digital outputs, thereby catering to a variety of sensor and control requirements during testing. The user interface of this board is both compact and efficient, incorporating a 1.3" OLED display alongside three tactile buttons for straightforward operation and real-time monitoring.

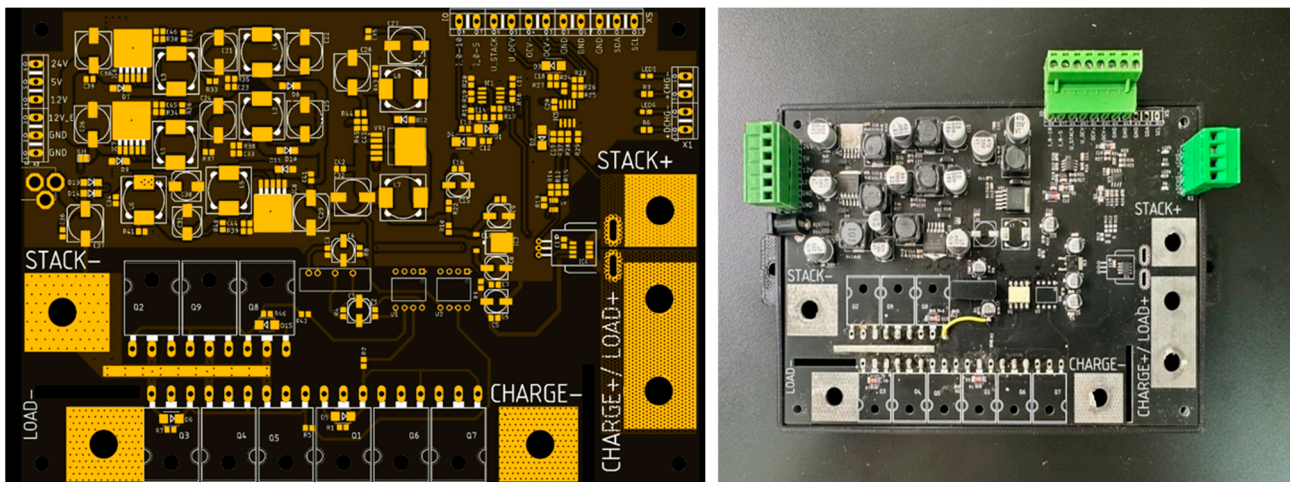


Figure 1. The PCB layout of the power module.

Data monitoring and control are elevated to a new level of convenience and efficiency with the integration of a Nodered server (Figure 2). This server collects and processes data from the testing module, presenting it on a user-friendly Nodered dashboard. Users can access and control the testing parameters through this dashboard, enabling remote monitoring and adjustment of the charge/discharge cycles. This advanced feature not only enhances the usability of the testing module but also allows for more sophisticated and nuanced experimentation with redox flow battery systems.

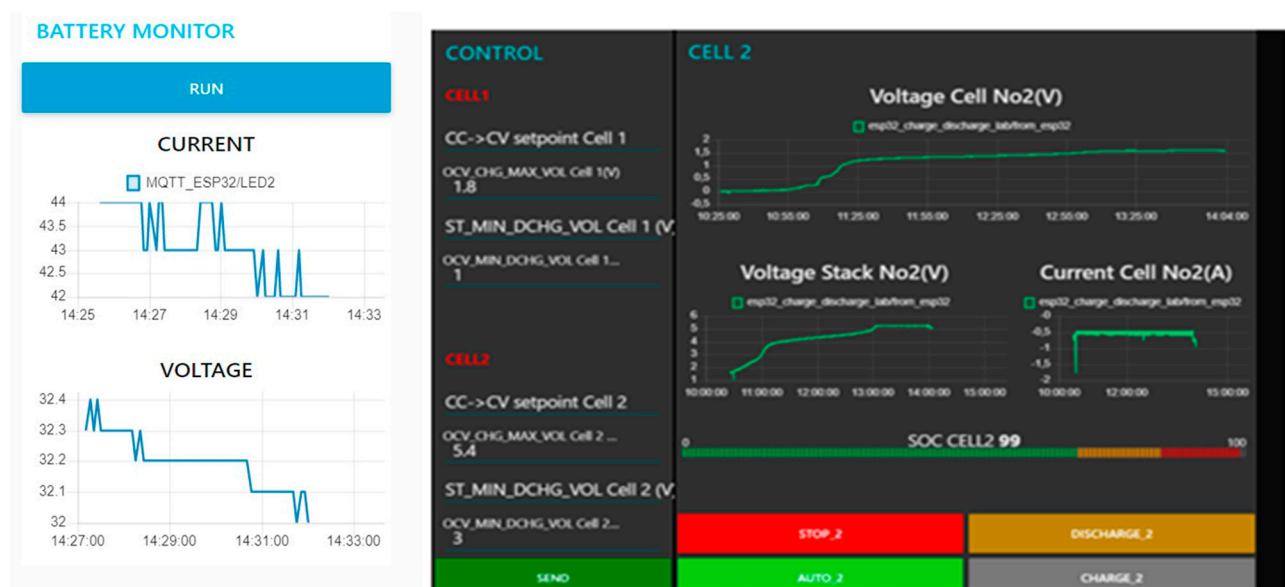


Figure 2. The Nodered dashboard used to control and monitor the charge/discharge module.

The research team have designed and provide all the schematics, along with Gerber files of the charge/discharge system in the Supporting Information S1 (SI 1). This information allows other research groups to replicate and test the device. The setup instructions for the charge/discharge module are comprehensively detailed in the Supporting Information. Within the Supporting Information, users will find:

1. Detailed assembly instructions: these cover the integration of the power module board with the ESP32-IO connection board, along with the proper installation of all related components.
2. Connection guidelines: directions are given for connecting the power module to the programmable power source (PPS), ensuring accurate control and monitoring during charge/discharge processes.
3. Data monitoring and Nodered dashboard usage: specifics are provided on transmitting data to the Nodered server and utilizing the Nodered dashboard for the effective control and observation of the module's functions.
4. Safety protocols: essential safety precautions and operational best practices are detailed to ensure the safe and reliable use of the charge/discharge testing module.

2.4. Rotating Electrodes

Rotating electrodes are essential in redox flow battery (RFB) research, particularly in the field of electrochemistry, where they provide controlled and consistent conditions for studying the kinetics and mechanisms of electrochemical reactions. Rotating disc electrodes (RDEs) allow for precise control over the mass transfer of reactants and products at the electrode interface, as they facilitate the steady laminar flow of the electrolyte to the electrode's surface. However, the cost of commercially available rotating electrodes has been a major barrier to RFB research, especially for less well-funded research groups. Traditional RDE setups can be prohibitively expensive, frequently requiring thousands of dollars, making them impractical. This challenge has been addressed by Whittingham [20], who provided a solution for low-cost RDE, adopting an inventive approach that uses additive manufacturing techniques to significantly reduce production costs without sacrificing performance. The study shows that it is feasible to use low-cost electronics that are widely available, along with a filament that is primarily based on acrylonitrile butadiene styrene (ABS), bringing the total cost of the additively manufactured RDE system to less than 2% of a comparable commercial solution. However, there may be drawbacks as well, such as possible limitations in its material properties and precision compared to commercial counterparts and the requirement for previous experience with additive manufacturing techniques. Nevertheless, this development represents a significant step toward increasing accessibility to high-quality research equipment, which could change the landscape of RFB research and broader electrochemical research. The advantages of this approach include drastically reduced costs and the potential for customization to specific research needs.

Our research team has modified the rotating electrode design innovatively to enhance its compatibility with the Opensens potentiostat, a key instrument in electrochemical analysis. This modification involves incorporating two layers of carbon brushes, one for the working electrode (WE) and another for the sensing electrode (SE). This dual-brush configuration plays a critical role in stabilizing electrochemical measurement, particularly by eliminating the signal drift that occurs during scanning (Figure 3c,d). Signal drift, a common issue in electrochemical experiments, can lead to inaccuracies in the interpretation of reaction kinetics and mechanisms. The setup instructions for the rotating electrode module are comprehensively detailed in Supporting Information S2 (SI 2).

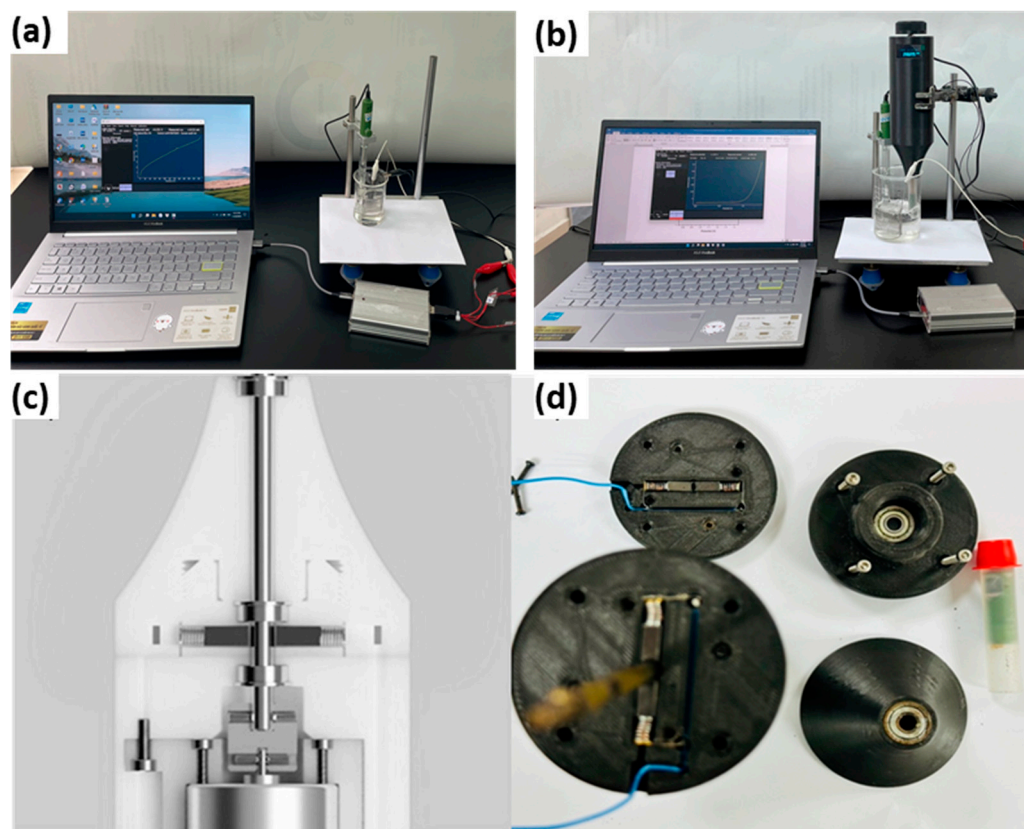


Figure 3. (a) The setup used for the CV experiments, (b) the experimental setup of the RDE and Opensens used in the experiments, (c) the original design with a one-brush electrode, and (d) the dual-brush electrode.

The initial design concepts of rotating electrodes commonly employ direct current (DC) motors to accomplish the necessary rotation. Nevertheless, within the realm of RFB research, a transition occurred toward the utilization of stepper motors in such electrode designs. Stepper motors provide improved stability and accuracy, both of which are vital for conducting precise electrochemical measurements. Moreover, they enable more regulated and precise rotational velocities, a critical factor when investigating the dynamic nature of the electrodes. The necessary files for generating these prints are accessible in the Supporting Information S1 (SI 1). A notable drawback of this novel design employing stepper motors is a restricted maximum rotational speed of 3000 revolutions per minute (rpm). This constraint is substantial, given that specific electrochemical analyses may require higher speeds for enhanced mass transfer rates at the electrode's surface, which are vital for investigating faster electrochemical reactions. Nevertheless, the improved stability and precision offered by the capped speed offset this drawback.

For this experimental setup involving rotating disk electrodes (RDEs) and the Opensens potentiostat, a standard divided three-electrode glass cell was employed for the cyclic voltammetry experiments. The electrolyte temperature was meticulously maintained at 30 °C. When studying cerium half-cell reactions, RDEs served as the working electrodes, while a platinized titanium mesh was utilized as the counter electrode (Figure 3b). The electrode's potential was accurately measured against a saturated calomel reference electrode, ensuring precise and reliable readings.

2.5. Electrolyte Preparation

This process involved preparing an electrolyte solution from V_2O_5 , oxalic acid, and H_2SO_4 . First, 91 g of V_2O_5 was dissolved in a stirred H_2SO_4 4 M solution at 40 °C, followed by the addition of oxalic acid in a 1:1 mole ratio with V_2O_5 . The resulting mixture, stirred

and heated until a blue coloration appeared, was then diluted over 24 h to achieve the desired concentration of vanadium 1 M. This electrolyte should be used in cells under a nitrogen atmosphere to prevent any oxidation reactions, employing specific charging modes to achieve solutions with predominant V^{2+} and VO_2^+ ions in the negative and positive compartments, respectively. To produce the Ce-catholyte, $Ce_2(CO_3)_3$ was dissolved into a mixture of deionized water containing a specific volume of 30% H_2O_2 , followed by adding a specific volume of methanesulfonic acid (MSA) solution. The mixture was stirred until the complete dissolution of the $Ce_2(CO_3)_3$ salt was achieved. Afterward, the solution was heated to 70 °C for 2 h to eliminate any excess H_2O_2 . A small sample of the solution was then mixed with a small amount of potassium iodide salt and a few drops of starch solution to confirm the complete removal of excess H_2O_2 . The solution was centrifuged at 6000 rpm to remove any undissolved solid impurities. Finally, set amounts of MSA and H_2SO_4 acids were gradually added to the solution under continuous stirring at 100 rpm for 1 h. Deionized water can be used to control the concentration of Ce^{3+} ions in the catholyte.

Cyclic voltammetry (CV) was performed at various scan rates from 5 $mV s^{-1}$ to 10 $mV s^{-1}$ to determine the reversibility of the catholyte and anolyte. The cyclic voltammograms of vanadium (IV/V) and cerium (III/IV) half-cells in mixed acid electrolytes were recorded, sweeping the potential in specified ranges at a scan rate of 20 mV/s using the flow cell (Table 1). Linear sweep voltammetry was carried out using a Pt rotating disk electrode (3 mm \varnothing); the rotating angular velocity ω was set from 100 to 900 rpm, and the electrode potential was swept at 5 $mV s^{-1}$. Pt wire was used as a counter electrode. An Ag/AgCl electrode was employed as a reference electrode. Electrochemical data were collected by our lab-made Opensens system [21].

3. Results and Discussion

3.1. The Cyclic Voltammograms of Vanadium (IV/V) and Cerium (III/IV) Half-Cells

An example of Opensens in use is shown in Figures 4 and 5, wherein cyclic voltammetry studies of redox flow batteries are being conducted. In Figure 4a, the cyclic voltammograms of a platinum electrode in 1 M of vanadium electrolyte with varying concentrations of H_2SO_4 demonstrate electrochemical behavior under different acidic conditions. Figure 4b further explores this by examining 0.6 M of cerium methane sulfonate with different concentrations of H_2SO_4 , illustrating the potential range and current response.

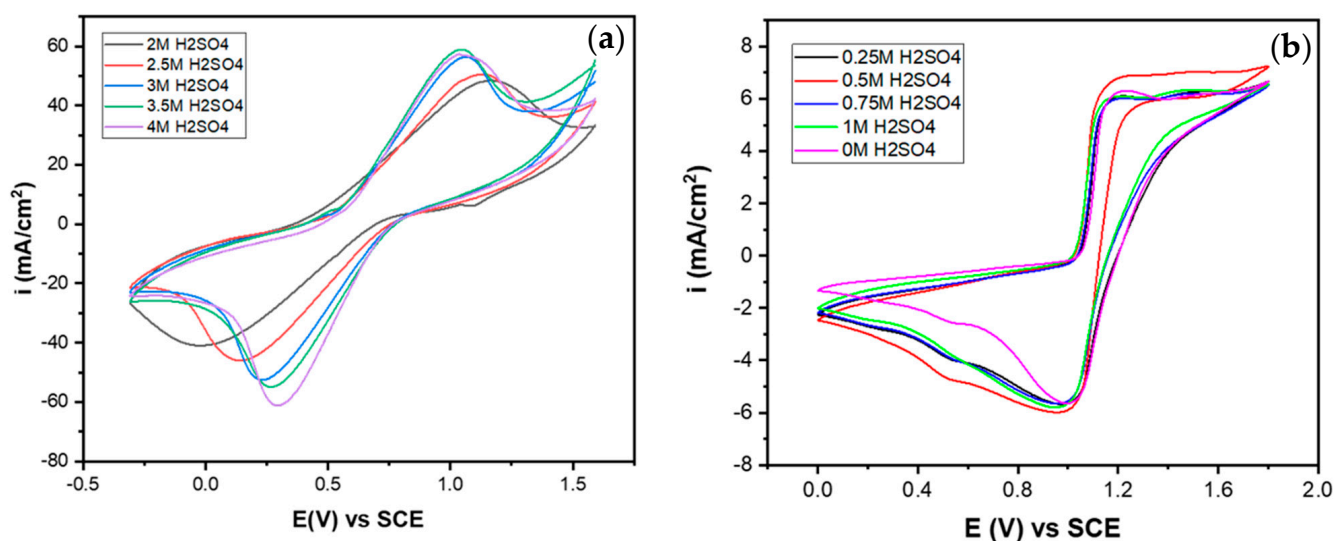


Figure 4. Cyclic voltammograms of a Pt electrode in: (a) 1 M of vanadium electrolyte with different concentrations of H_2SO_4 , (b) 0.6M $Ce(CH_3SO_3)_3$ + 4M MSA + x M H_2SO_4 .

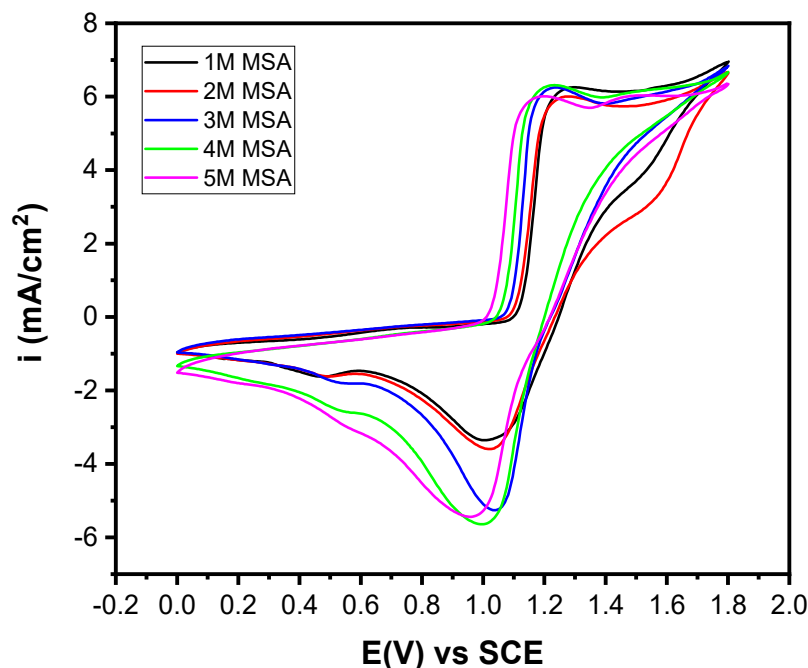


Figure 5. Cyclic voltammograms of a Pt electrode in 0.6 M $\text{Ce}(\text{CH}_3\text{SO}_3)_3 + x$ M MSA ($x = 1, 2, 3, 4, 5$).

The effect of methanesulfonic acid (MSA) concentrations on cerium-based electrolytes is demonstrated in Figure 5, highlighting how their electrochemical properties vary with acid concentration. These examples underscore the adaptability and effectiveness of Opensens in comprehensive electrochemical studies, providing a cost-effective and adaptable tool for advancing redox flow battery research.

3.2. The Linear Sweep Voltammetry of Electrolytes

Electrochemical measurements were conducted using an Opensens system. To analyze the cerium (III/IV) redox reaction, linear sweep voltammetry (LSV) was performed (Figure 6). This involved a linear sweep of the potential from 0.8 V to 1.4 V versus the calomel reference, at a scan rate of 10 mV/s. This methodical approach allowed for detailed observation and analysis of the electrochemical behavior of cerium in the specified potential range, providing valuable insights into its redox characteristics under controlled experimental conditions.

The electrochemical measurements were conducted using an Opensens potentiostat/galvanostat. To analyze the cerium (III/IV) redox reaction, linear sweep voltammetry (LSV) was performed. Figure 6 presents the linear sweep voltammetry (LSV) results of a 0.6 M $\text{Ce}(\text{CH}_3\text{SO}_3)_3 + 4\text{M}$ methanesulfonic acid (MSA) + 0.5 M $\text{H}_2\text{SO}_4 + 2\%$ mol L-Lysine electrolyte at varying rotation speeds, ranging from 100 to 900 rpm. The electrochemical measurements, conducted using the Opensens system, involve sweeping the potential from 0.8 V to 1.4 V versus a saturated calomel electrode (SCE) at a scan rate of 10 mV/s. The LSV curves illustrate the effect of rotation speed on the current response, showcasing the increased current density seen with higher rotation speeds, which is indicative of enhanced mass transport at the electrode's surface. The observed trends in the voltammograms reflect the kinetics of the cerium (III/IV) redox reaction, wherein higher rotation speeds lead to a sharper rise in current, highlighting the influence of convective mass transfer on the electrochemical behavior of the system. This detailed analysis of the cerium redox characteristics under varying hydrodynamic conditions provides significant insights into the efficiency and dynamics of the electrolyte, which are crucial for optimizing RFB performance.

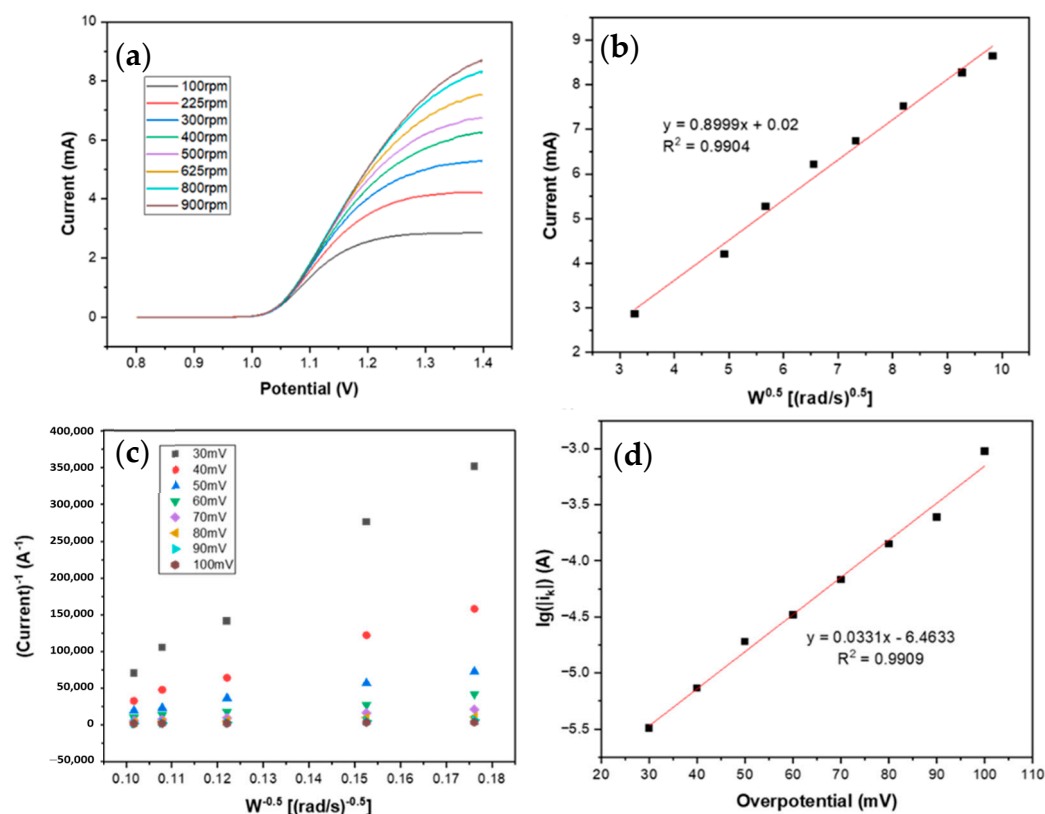


Figure 6. (a) Linear sweep voltammetry of 0.6 M $\text{Ce}(\text{CH}_3\text{SO}_3)_3$ + 4M MSA + 0.5 M H_2SO_4 + 2% mol L-Lysine electrolyte with different rotation speeds at a scan rate of 5 mV/s. (b) Levich plot of limiting current versus the square root of the rotation rate ($\omega^{1/2}$). (c) Koutecky–Levich plot at different overpotentials. (d) Tafel plot of the logarithm of kinetically limited current versus overpotential.

3.3. Full-Cell Charge/Discharge Battery Testing

Figure 7 illustrates the charge and discharge curves of the V-Ce flow battery with a concentration of 1 M for both vanadium and cerium ions (V and Ce^{3+} , respectively). The current during charging is maintained at 0.05 A; during discharging, it is maintained at -0.05 A. The voltage is limited to within the range of 2 V and 0.6 V. As Figure 7 shows, voltage does not continuously increase; however, with more charge/discharge cycles, the voltage begins increasing continuously. Normally, this phenomenon is specific for single and small RFB cells because of the effect of liquid flows during the pumping process. In addition, the system is homogeneously low for several of the first cycles, which could be due to the interaction of the electrolytes (both catholyte and anolyte) with electrodes and also the time needed for stabilizing redox pairs in the catholyte and anolyte. By combining various RFB stacks and/or by using big RFB cells, this issue should be resolved and the voltage should be increasing continuously [1,2,6,9,10].

Figure 8 illustrates the efficiency of a redox flow battery over 9 cycles, focusing on energy efficiency, Coulombic efficiency, and voltage efficiency. The Coulombic efficiency value remains consistently high at around 90%, indicating efficient charge storage and retrieval processes with minimal side reactions. Both energy and voltage efficiencies stabilize between 50% and 60% after the initial cycles, demonstrating stable operation over time, despite moderate inefficiencies. The voltage efficiency, reflecting losses due to overpotentials and internal resistance, is notably lower than the Coulombic efficiency, highlighting voltage-related losses as a key area for improvement. Potential enhancements include reducing the internal resistance through better electrolyte conductivity and electrode design, optimizing redox reactions to minimize overpotential, and employing advanced materials for the electrodes and membranes to improve overall efficiency and battery lifespan.

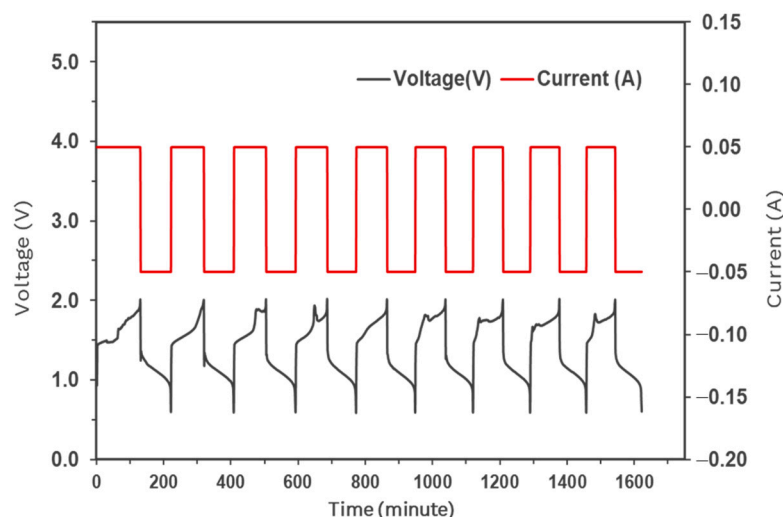


Figure 7. Charge/discharge curves of the V-Ce RFB (current $I = 0.05$ A, with voltage limits at 2.0–0.6 V).

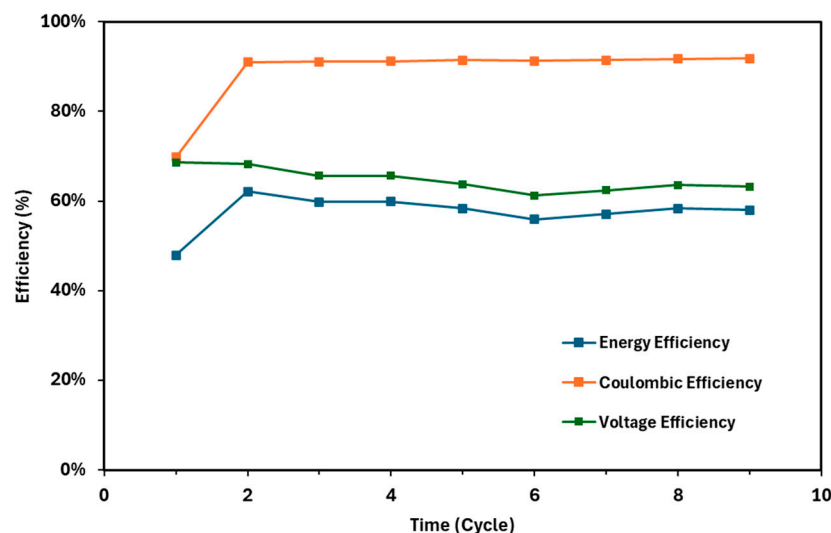


Figure 8. Coulombic, voltage, and energy efficiency as a function of the cycle number.

4. Conclusions

This study underscores the pivotal role of open-source methodologies in advancing research into RFBs. By offering comprehensive designs and fabrication guidelines for various flow cells at a substantially lower cost, this study highlights the practicality and efficacy of these accessible alternatives. Their successful charge and discharge performance further substantiates the real-world applicability of these open-source designs. A major contribution of this work is the development of custom devices tailored to overcome the constraints of commercial equipment. While commercial solutions are typically suited for small-area electrode applications, the higher current demands of larger electrode areas necessitate purpose-built equipment. This distinction underscores the adaptability and essential nature of bespoke solutions in RFB research. Furthermore, this study demonstrates the utility of open-source electrochemical instruments, such as the Opensens potentiostat/galvanostat and 3D-printed rotating disc electrodes. These tools not only lower operational costs but also improve the precision and reliability of electrochemical measurement. Their deployment in this research exemplifies how open-source technologies can revolutionize the future of RFB research, fostering greater inclusivity and driving innovation in the pursuit of sustainable energy storage solutions. The open-source framework presented in this study

is positioned to accelerate technological progress in RFBs, facilitating the integration of renewable energy and contributing to efforts to mitigate climate change.

Supplementary Materials: The following supporting information can be downloaded at: <https://www.mdpi.com/article/10.3390/chemengineering8060120/s1>, Supporting Information S1 (SI 1): The charge/discharge testing device. Supporting Information S2 (SI 2): The rotating disk electrode.

Author Contributions: T.V.D., N.T.T.H., N.T.B., N.T.D., N.T.T.N., N.T.L. and N.T.T.M.: Investigation, writing—original draft, and data curation. N.L.T.H.: Investigation, data curation, and visualization. H.V.T.: Review and editing. C.D.H.: Supervision and writing—review. All authors have read and agreed to the published version of the manuscript.

Funding: This research is funded by the Vietnam Ministry of Education and Training (MOET) under grant number CT2022.04.BKA.05.

Data Availability Statement: The original contributions presented in the study are included in the article/Supplementary Materials; further inquiries can be directed to the corresponding author.

Conflicts of Interest: The authors declare no conflicts of interest.

References

1. Liu, B.; Li, Y.; Jia, G.; Zhao, T. Recent Advances in Redox Flow Batteries Employing Metal Coordination Complexes as Redox-Active Species. *Electrochem. Energy Rev.* **2024**, *7*, 7. [CrossRef]
2. Venkatesan, S.V.; Nandy, A.; Karan, K.; Larter, S.R.; Thangadurai, V. Recent Advances in the Unconventional Design of Electrochemical Energy Storage and Conversion Devices. *Electrochem. Energy Rev.* **2022**, *5*, 16. [CrossRef]
3. Panwar, N.L.; Kaushik, S.C.; Kothari, S. Role of renewable energy sources in environmental protection: A review. *Renew. Sustain. Energy Rev.* **2011**, *15*, 1513–1524. [CrossRef]
4. Gür, T.M. Review of electrical energy storage technologies, materials and systems: Challenges and prospects for large-scale grid storage. *Energy Environ. Sci.* **2018**, *11*, 2696–2767. [CrossRef]
5. Pacific Northwest National Laboratory. Redox Flow Battery Laboratories. Available online: <https://www.pnnl.gov/redox-flow-battery-laboratories> (accessed on 13 September 2024).
6. Skyllas-Kazacos, M.; Chakrabarti, M.H.; Hajimolana, S.A.; Mjalli, M.S.F.S. Progress in Flow Battery Research and Development. *J. Electrochem. Soc.* **2011**, *158*, R55. [CrossRef]
7. Sánchez-Díez, E.; Ventosa, M.G.E.; Trovò, A.; Flox, C.; Marcilla, R.; Soavi, F.; Mazur, P.; Aranzabe, E.; Ferret, R. Redox flow batteries: Status and perspective towards sustainable stationary energy storage. *J. Power Sources* **2021**, *481*, 228804. [CrossRef]
8. Ke, X.; Alexander, J.I.D.; Savinell, R.F. Redox flow batteries with serpentine flow fields: Distributions of electrolyte flow reactant penetration into the porous carbon electrodes and effects on performance. *J. Power Sources* **2018**, *384*, 295–302. [CrossRef]
9. Weber, A.Z.; Mench, M.M.; Meyers, J.P.; Ross, P.N.; Gostick, J.T.; Liu, Q. Redox flow batteries: A review. *J. Appl. Electrochem.* **2011**, *41*, 1137–1164. [CrossRef]
10. Wang, W.; Luo, Q.; Li, B.; Wei, X.; Li, L.; Yang, Z. Recent Progress in Redox Flow Battery Research and Development. *Adv. Funct. Mater.* **2013**, *23*, 970–986. [CrossRef]
11. Yu, V.; Chen, D. Dynamic Model of a Vanadium Redox Flow Battery for System Performance Control. *J. Sol. Energy Eng.* **2014**, *136*, 021005. [CrossRef]
12. YChen, S.; Ho, S.-Y.; Chou, H.-W.; Wei, H.-J. Modeling the effect of shunt current on the charge transfer efficiency of an all-vanadium redox flow battery. *J. Power Sources* **2018**, *390*, 168–175.
13. Leung, P.; Li, X.; de Leon, C.P.; Berlouis, L.; Low, C.T.J.; Walsh, F.C. Progress in redox flow batteries, remaining challenges and their applications in energy storage. *RSC Adv.* **2012**, *2012*, 10125–10156. [CrossRef]
14. Chen, H.; Cong, G.; Lu, Y. Recent progress in organic redox flow batteries: Active materials, electrolytes and membranes. *J. Energy Chem.* **2018**, *27*, 1304–1325. [CrossRef]
15. C-Tech Innovation. C-Flow 5 × 5 Electrochemical Cell. Available online: <https://www.ctechinnovation.com/product/c-flow-5x5/> (accessed on 13 September 2024).
16. Biologic, Redox Flow Battery Cells. Available online: <https://www.biologic.net/accessory/redox-flow-battery/> (accessed on 13 September 2024).
17. Redox-Flow. Redox Flow Battery Test Cell. Available online: <https://redox-flow.com/products/redox-flow-battery-test-cell> (accessed on 13 September 2024).
18. MTI Corporation. Vanadium Redox Flow Cell (Single Split Unit) for Battery R&D-EQ-VRB-C-LD. Available online: <https://www.mtixtl.com/VanadiumRedoxFlowCellSingleSplitUnitforBatteryRandD-EQ-VRB-C-LD.aspx> (accessed on 13 September 2024).
19. O'Connor, H.; Bailey, J.J.; Istrate, O.M.; Klusener, P.A.A.; Watson, R.; Glover, S.; Iacoviello, F.; Brett, D.J.L.; Shearing, P.R.; Nockemann, P. An open-source platform for 3D-printed redox flow battery test cells. *Sustain. Energy Fuels* **2022**, *2022*, 1529–1540. [CrossRef]

20. Whittingham, M.J.; Crapnell, R.D.; Banks, C.E. Additively Manufactured Rotating Disk Electrodes and Experimental Setup. *Anal. Chem.* **2022**, *94*, 13540–13548. [[CrossRef](#)] [[PubMed](#)]
21. Trinh, V.D.; Le, M.K.; Le, P.L.; Ho, A.T.; Nguyen, H.A.; Thai, T.T.; Hoang, T.B.T.; Nguyen, T.T.H.; Huynh, L.T.N.; Huynh, D.C. OPENSENS: A low cost and multi purpose electrochemical platform. *J. Appl. Electrochem.* **2024**, *54*, 783–789. [[CrossRef](#)]

Disclaimer/Publisher's Note: The statements, opinions and data contained in all publications are solely those of the individual author(s) and contributor(s) and not of MDPI and/or the editor(s). MDPI and/or the editor(s) disclaim responsibility for any injury to people or property resulting from any ideas, methods, instructions or products referred to in the content.